Childs Nerv Syst (2013) 29:597–607
DOI 10.1007/s00381-012-1973-8

ORIGINAL PAPER

Fronto-cerebellar fiber tractography in pediatric patients following posterior fossa tumor surgery

Verena Soelva · Pablo Hernáiz Driever · Alexander Abbushi · Stefan Rueckriegel · Harald Bruhn · Wilhelm Eisner · Ulrich-Wilhelm Thomale

Received: 3 September 2012 / Accepted: 13 November 2012 / Published online: 27 November 2012

Abstract
Objective Fronto-cerebellar association fibers (FCF) are involved in neurocognitive regulatory circuitry. This may also be relevant for cerebellar mutism syndrome (CMS) as a complication following posterior fossa tumor removal in children. In the present study, we investigated FCF by diffusion tensor imaging in affected children and controls.
Methods Diffusion-weighted MR imaging at 3 T (GE) allowed tractography of FCF using a fiber tracking algorithm software (Brainlab 2.6) in 29 patients after posterior fossa tumor removal and in 10 healthy peers. Fiber tract volumes were assessed and fiber signals were evaluated in a semiquantitative manner along the anatomical course.
Results Volumes of FCF revealed significant diminished values in pediatric patients with symptoms of CMS (19.3± 11.7 cm^3) when compared with patients without symptoms of CMS (26.9±11.9 cm^3) and with healthy peers (36.5± 13.82 cm^3). In medulloblastoma patients, the volume of FCF was also significantly reduced in patients with symptoms of CMS despite having the same antitumor therapy. In semiquantitative analysis of the fiber tract signals, differences were observed in the superior cerebellar peduncles and midline cerebellar structures in patients with symptoms of CMS.
Conclusion Using DTI, which allows the visualization of fronto-cerebellar fiber tracts, lower FCF tract volumes and diminished fiber signal intensities at the level of the superior cerebellar peduncles and in midline cerebellar structures were identified in patients with postoperative symptoms of CMS. Our study refers to the role of a neural circuitry between frontal lobes and the cerebellum being involved in neurocognitive impairment after posterior fossa tumor treatment in children.

Keywords Diffusion tensor imaging · Tractography · Pediatric brain tumor · Posterior fossa surgery · Cerebellar mutism

V. Soelva · A. Abbushi · U.-W. Thomale (✉)
Arbeitsbereich Pädiatrische Neurochirurgie,
Charité-Universitätsmedizin Berlin, Campus Virchow Klinikum,
Augustenburger Platz 1,
13353 Berlin, Germany
e-mail: uthomale@charite.de

P. Hernáiz Driever · S. Rueckriegel
Klinik für Pädiatrie mit Schwerpunkt Onkologie und Hämatologie,
Berlin, Germany

H. Bruhn
Radiologie, Charité-Universitätsmedizin Berlin, Berlin, Germany

W. Eisner
Neurochirurgische Klinik, Medizinischen Universität Innsbruck,
Innsbruck, Austria

Introduction

Mutism is defined as the absence of speech in an awake and conscious patient with intact comprehension and was first described by Rekate [11, 16, 24]. Cerebellar mutism syndrome (CMS) is a frequently described complication following posterior fossa tumor removal. It is characterized as a disturbance of neuropsychological function leading to diminished impulsion associated with inhibition of speech output and may be associated with posterior fossa syndrome (PFS) that includes ataxia, muscular hypotonia, hemi- or tetraparesis, and possible cranial nerve deficits [11, 25, 35]. Complete presence of cerebellar mutism is a differential diagnosis of a comatose state while incomplete symptomatology is associated with behavioral changes such as emotional lability and irritability [11, 25]. This condition is more often seen in the pediatric population and has rarely been reported in young adults [5]. The incidence of postoperative CMS ranges from 8 % to 29 %. It may manifest either

immediately or with a delay of 1 to 2 days after surgery. The duration of CMS is largely variable and believed to be reversible in most cases [5, 10, 11, 16, 25, 34]. Still, a relevant number of children may develop a lasting cerebellar cognitive affective syndrome [29]. Intraoperative damage as well as postoperative disturbances, i.e., vasospasm or edema, may play a causative role [34]. The anatomical structures most prone to injury associated with CMS are cerebellar midline structures, dentate nucleus, and the dentato-thalamo-cortical outflow tracts [4, 6, 23]. Risk factors to develop CMS are midline tumors or brainstem involvement, tumor size, and tumor type, as it occurs more often in medulloblastoma patients. Inconsistent risk factors as described in the literature are radical tumor removal and vermal incision [2, 9, 10, 16, 25]. Earlier studies applied different imaging techniques in order to elucidate the pathophysiologic understanding of the development of CMS. Single photon emission tomography (SPECT) revealed inconsistent findings of local hypoperfusion in mute patients after posterior fossa surgery [7, 9, 20]. In different MRI investigations, ischemia, edema, and structural damage of midline structures were described as contributing factors [4, 18, 23]. Since children are significantly more prone to develop CMS after posterior fossa surgery and younger age resulted in poorer outcome, developmental factors have been hypothesized to play a role such as a specific pathology of neuronal lesion to incompletely myelinated pathways [21, 26]. As an anatomical substrate for white matter lesions, dentate-thalamico-cortical (DTC) outflow tracts originating from cerebellar nuclei have been supposedly affected in cases of CMS [18, 25]. Therefore, analyses of white matter tracts may lead to further insight in CMS.

Diffusion tensor MR imaging (DTI) has been already used to identify white matter lesions in patients suffering posterior fossa syndrome. Significantly reduced fractional anisotropy (FA) values were identified in DTC pathways [18]. Similarly, generation of FA maps using tract-based spatial statistics showed damage to supratentorial white matter microstructures in pediatric cerebellar tumor survivors with or without adjuvant therapy [27]. Thus, DTI seems to be a valuable tool for investigation of CMS in pediatric neurosurgical patients.

Similar symptoms of mutism may be observed in patients with bifrontal lobe dysfunction after, e.g., trauma, tumors, epilepsy, or stroke leading to speech deficits such as akinetic mutism and verbal adynamia [14, 17, 19, 32]. As a new concept, we hypothesized that damage to white matter tracts connecting the cerebellum and the frontal lobes, further defined in general as fronto-cerebellar association fibers (FCF), are involved in the development of CMS. We aimed to visualize FCF by using DTI for tractography in pediatric posterior fossa tumor survivors and compared them with healthy peers. We asked whether the presence of clinical postoperative symptoms or the tumor diagnosis correlated with FCF integrity.

Patients and methods

Subjects

In a cross-sectional study of 29 pediatric posterior fossa tumor survivors (13 girls) and 10 healthy peers who underwent diffusion-weighted imaging (3-T MRI, Signa; GE) we performed tractography of FCF by using a fiber tracking algorithm software (tool—brain Lab 2.6; Brainlab, Germany). Patients underwent surgery between July 1998 and June 2006 (median, May 2005; mean age, 9±4.3 years). Mean time between surgery and imaging was 2.5±1.9 years (range, 0.2–8.1). A group of 10 healthy peers (four girls) were investigated accordingly. Their mean age was 12.9± 3.8 years, which was higher than in patients due to difficulties to obtain MRI scans of children younger than 6 years of age in the healthy peer group. The local institutional ethical review board approved the MRI studies. All individuals and/or their parents gave a written, informed consent. The patient cohort was selected as consecutive patients from the oncology outpatient clinic during follow-up investigations and according to their consent for the study.

Fourteen patients suffered from pilocytic astrocytoma WHO grade I, 13 from medulloblastoma, and two from ependymoma (one WHO grade II and one grade III). The tumor localization in the presented cohort revealed fourth ventricular (n=16), paramedian (n=10), and lateralized (n=3) localization. The lateralization in the latter two groups revealed 10 left-sided and three right-sided tumors. All medulloblastoma patients and one ependymoma patient (WHO grade III) received in addition to surgery adjuvant chemotherapy and radiation. The second ependymoma patient received postoperative radiation alone. Adjuvant treatments were performed according to approved HIT 2000 protocol of the German Speaking Society of Pediatric Oncology and Hematology (GPOH).

Fig. 1 Analysis of fiber tracts was performed by using the iPlan 2.6 software tool (BrainLab). Minimal length of fibers was set at 70 mm; fractional anisotropy (FA) threshold of 0.1 was applied. As starting region of interest (ROI), the prefrontal cortex was chosen, including a volume delineated by the frontal cerebral pole, the interhemispheric fissure, and the temporal pole (**a**, *upper pictures*). As target ROI, a cubic volume was set that included the entire cerebellum (**a**, *lower pictures*). Due to possible overlaps of the cubic ROIs with neighboring structures (corner areas involving e.g. the occipital lobe in the target ROI), erroneously tracked fiber streamlines that did not enter the frontal lobe or the cerebellum were carefully erased by using an exclusion algorithm which is integrated in the software tool (**b**)

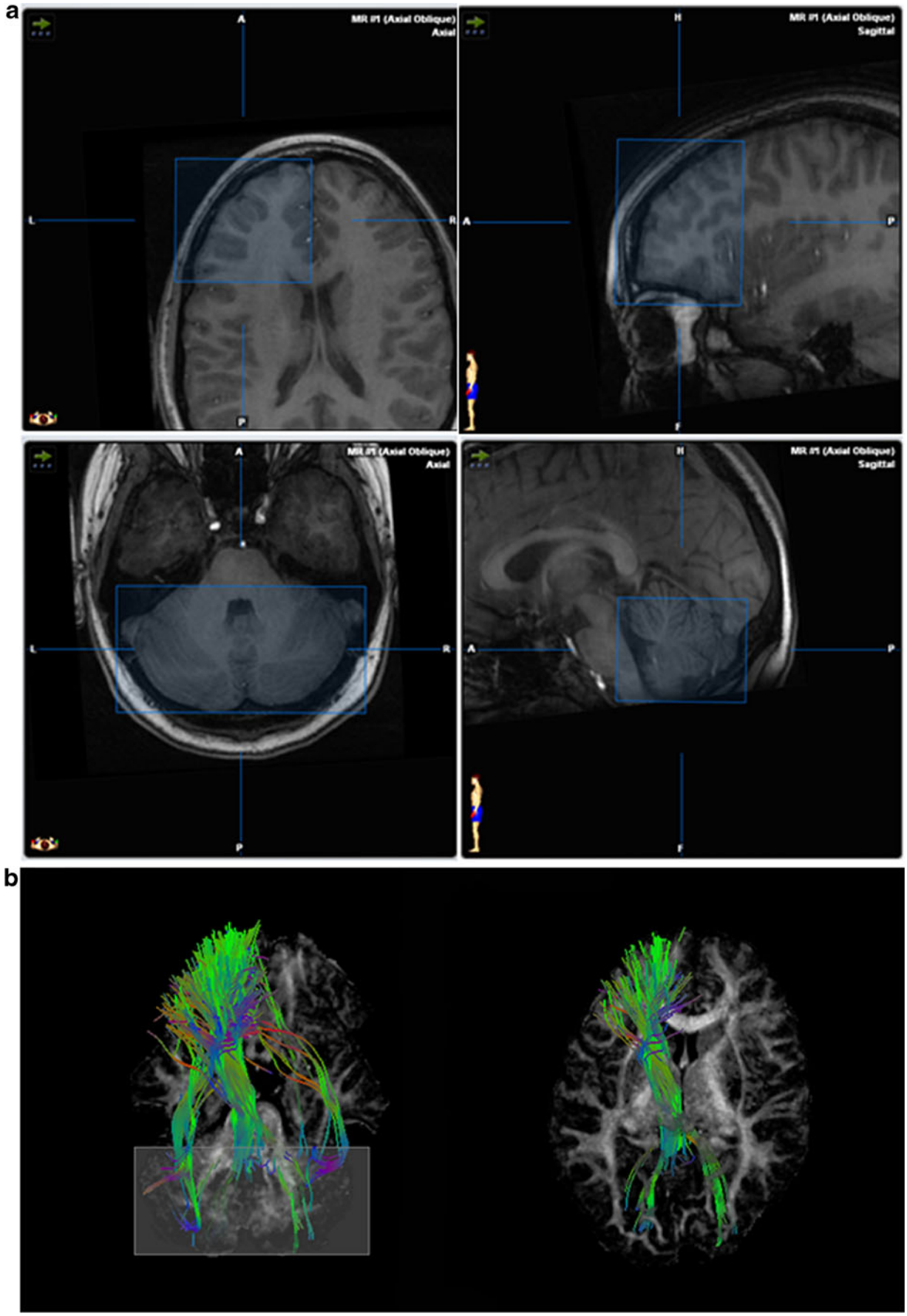
a
MR #1 (Axial Oblique)
Axial
MR #1 (Axial Oblique)
Sagittal
b

Patients were divided into two different groups, depending on clinical outcome, according to a modified grading system presented by Robertson et al. [25]. Postoperative clinical symptoms were classified into primary and secondary symptoms of posterior fossa syndrome (PFS) which were documented in the medical reports within the first week after surgery. Primary symptoms were defined as ataxia, any behavioral changes, and the complete appearance of CMS. Secondary symptoms were defined as cranial nerve dysfunctions. Group A represented patients with either unremarkable postoperative clinical course, only ataxia as primary symptom, and/or only secondary symptoms. In contrast, group B patients had postoperatively developed at least two of the primary symptoms of PFS up to complete CMS with or without secondary symptoms. Mean age was 9.2±4.4 years in group A (n=18) and 8.7±4.4 years in group B (n=11). Mean time period between scanning and surgery was 2.6±1.8 years and 2.3±2.1 years, respectively. Eight out of 13 of medulloblastoma patients developed two or more primary symptoms and were classified to group B. Two out of 14 pilocytic astrocytoma patients and one of the two ependymoma patients fulfilled the criteria of group B.

Diffusion tensor imaging (DTI)

Diffusion tensor imaging may provide information on the integrity of the microstructural organization of brain tissue in vivo. The translational movement of water molecules is limited by the presence of boundaries like the myelin sheaths or cell membranes [15]. Measuring the preferred direction of water diffusion, DTI can detect the orientation of white matter fibers because water molecules diffuse along the longitudinal axis of axons in an anisotropic (directional) pattern rather than isotropic (multidirectional) [31]. Thus, the direction of the fastest diffusion indicates the orientation of space in a fiber [15]. With a multidimensional MR diffusion tensor dataset and using an analytical algorithm, the spatial orientation of diffusion anisotropy can be depicted. The method was employed to map the orientation of white matter tracts in the brain using a color scale for visualization (red for left–right, green for antero-posterior, and blue for cranio-caudal) [15].

DTI protocol

All MRI data were acquired on a whole-body 3-Tesla MR scanner (Signa Excite; GE Healthcare, Waukesha, WI, USA) using the eight-channel phased-array headcoil of the manufacturer. Diffusion tensor MRI employing single-shot spin echo-planar imaging [repetition time (TR)/echo time (TE)=9,000 ms/100 ms] was performed with a parallel acceleration factor of 2 using the "array spatial sensitivity encoding technique (ASSET)". The diffusion gradients were applied in 25 directions at a b-factor of 1,000. An additional image set was acquired without the use of diffusion gradients (b=0). The whole brain was covered with a stack of 25–28 contiguous sections of 4 mm and an in-plane resolution of 1 mm×1 mm resulting in a total of 650–728 images acquired in approximately 5 min. Anatomic MRI included three-dimensional inversely prepared fast spoiled gradient-echo imaging (3DFSPGR) with isotropic voxels of 1-mm resolution primarily acquired in sagittal orientation and approximately 8-min scan time. Second, for diagnostic purposes conventional axial T2-weighted fast spin echo imaging (TR/TE, 4,000 ms/100 ms; 3-mm sections) was included as well as T1-weighted inversion-recovery fast spin echo sequences (TR/TE, 2,000 ms/15 ms, inversion time 860 ms; 5-mm sections, in-plane resolution 0.4 mm×0.8 mm). The 3D gradient-echo data were entered as anatomic correlates for image fusion in the Brainlab software tool (iPlan 2.6), while the DTI data enabled specific analysis of fronto-cerebellar-association fibers.

For processing the acquired data in iPlan 2.6, the 3D data had to be converted into a compatible format using PatXfer 5.2, a part of the Brainlab software tool. Then, two independent investigators (VS and AA) performed the DTI analysis protocol for fronto-cerebellar fiber tracking. The software tool iPlan 2.6 automatically fused the image data sets, which were individually verified for consistency and if necessary manually adapted along the anatomical landmarks of the ventricular structures the brainstem and the cerebellum. For the analysis of fiber tracts, the minimal length of tracked fibers was set as 70 mm, while a fractional anisotropy (FA) threshold of 0.1 was set in all subjects to visualize fronto-cerebellar fibers. As starting regions of interest (ROI) or "seed location", the prefrontal cortex was chosen, including a volume delineated by the frontal cerebral pole, the interhemispheric fissure, and the temporal pole (Fig. 1a). As target ROI, we defined a cubic volume that included the entire cerebellum (Fig. 1a). Due to possible overlaps of the cubic ROIs with neighboring structures (corner areas, e.g., occipital lobe in target ROI), erroneously tracked fiber streamlines that did not enter the frontal lobe or the cerebellum were carefully erased by using an exclusion algorithm which is integrated in the software tool (Fig 1b). The data collection of fronto-cerebellar fibers thus obtained was stored as sectional images and volumetric tracts for further analysis.

Analysis of fiber tracts

For volumetric analysis, the acquired fiber tracts were transformed into volumetric objects and measured in cubic centimeter with the iPlan 2.6 software (Fig. 2). For description of anatomic fiber localization, image sections were analyzed using supratentorial axial images. Infratentorial structures were investigated using coronal sections. A three-point rating scale was established to analyze the fiber signal in each section as a semiquantitative measure performed independently by two investigators (VS and AA). Scores of 0, 1, and 2 were assigned according to the amount of fiber signals in the anatomic

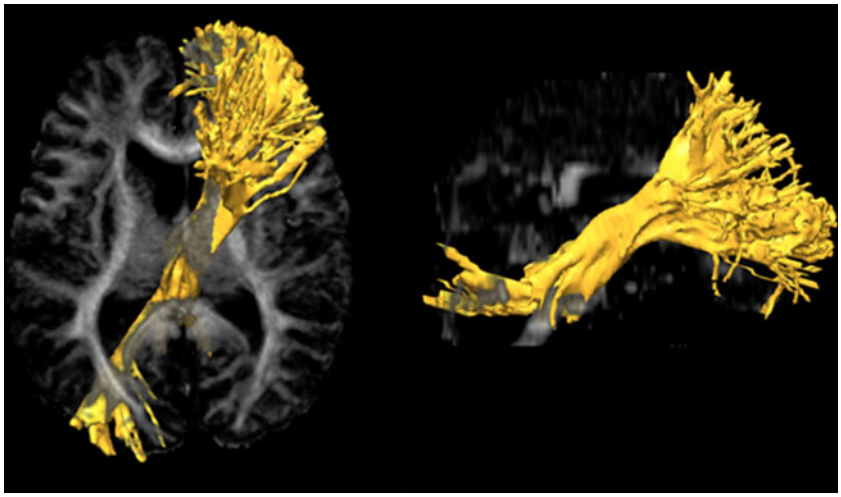

Fig. 2 Volumetric segmentation of fronto-cerebellar tracts originating from the left frontal lobe targeting the cerebellum with more distinct involvement of the right cerebellar hemisphere

structure in the respective section. The score of 2 was given for signals involving a distinct area within the anatomic structure. A score of 1 was given if there was a signal involving only minimal parts, while 0 was given in cases where no fiber signal was observed in the studied anatomic structure.

The anatomic regions of the fronto-cerebellar fiber course were evaluated as follows: the vascular territory of the frontopolar and frontal anteromedial artery, divided by the different gyri, i.e., superior frontal, medial frontal, and rectus; the anterior limb and knee of the internal capsule; the thalamus; the cerebral peduncles, the tegmentum and the pons, the superior and middle cerebellar peduncles as well as the cerebellum subsequently divided into lateral and medial structures.

In order to study the integrity of white matter structures within relevant areas of significant semiquantitative signal differences such as the superior cerebellar peduncles and the medial structures of the cerebellum, the anatomical structures were segmented and the FA values were determined using the iPlan 3.0 software tool.

Statistical analysis

All values were given as means with standard deviation. Statistical analysis were completed with GraphPad Prism 5.0 (GraphPad Software Inc., La Jolla, CA, USA) using one-way ANOVA followed by a post hoc analysis to compare possible statistical differences between the different patient groups as well as the control group. The level of statistical significance p was set <0.05.

Results

Patient characteristics

Eighteen patients were assigned to group A (no symptoms of CMS) and 11 to group B (symptoms of CMS). Eight out 13 of the medulloblastoma patients were classified to group B, while five medulloblastoma patients presented with complete postoperative signs of CMS compared to three medulloblastoma patients who had incomplete symptoms of CMS. In contrast, two out of 14 pilocytic astrocytoma patients were graded within group B with at least behavioral symptoms; however, no astrocytoma patient showed complete symptomatology of CMS. One patient with an ependymoma was classified to group A and the other to group B. According to the tumor localization, the symptoms CMS were more significantly associated with the fourth ventricle in 12 out of 16 cases compared to the paramedian localization (three out of 10 cases) and the lateral localization (one out of three cases). Twenty-four of the patients had tumor surgery before 10/2005 when the division of Pediatric Neurosurgery was founded at the Charité.

Anatomical course of FCF

Fronto-cerebellar fiber pathways were visualized bilaterally in all 10 healthy peers and 29 patients. In most subjects, FCF ran from the vascular territory of the frontopolar artery and the frontal anteromedial artery in the superior, medial, and straight gyrus of the frontal lobe in occipito-caudal direction through the anterior limb of the internal capsule into the thalamus. From here on, the fibers started to cross to the contralateral hemisphere. This was seen in all but one of the individuals. The supratentorial region of crossing fibers was mostly represented by the interthalamic adhesion where 42.1 % of patients and 30 % of healthy controls showed early contralateral fiber pathways. Most pronounced pathway crossings were seen in the tegmentum and pons and some were seen within the cerebellum. Fibers passed towards the tegmentum and the pons, and reached the cerebellum through the superior and middle cerebellar peduncles. The anatomical distribution of FCF within the cerebellar peduncles and the cerebellar hemispheres were compared between healthy peers and the patient group. In the healthy peer group, 100 % of fibers were

detected in the superior cerebellar peduncles and 90 % in the superior and the middle cerebellar peduncles. Similarly, in all patients the distribution of fibers was visualized in 100 % in the superior cerebellar peduncle. In 93 %, they were seen in both the superior and middle peduncles. Fiber signals of FCF were not seen in the inferior cerebellar peduncles, neither in patients nor in the control group.

Volume measurements of fronto-cerebellar fiber tracts

Volume measurements are given in Table 1. Volumes of FCF of patients in group B towards the left cerebral hemisphere were significantly smaller than those of healthy peers (17.59±9.36 cm^3 vs. 37.17±8.46 cm^3, $p<0.001$). Similarly, volumes of left and right FCF together in group B were significantly smaller than those of healthy peers (19.29±11.68 cm^3 vs. 36.47±13.82 cm^3; $p<0.001$). Differences of FCF volumes between patients of group A and B did not differ (Fig. 3).

In terms of histology, we found significantly smaller volumes when analyzing left FCF volumes in both pilocytic astrocytoma patients (23.43±9.34 cm^3) as well as in medulloblastoma patients (21.71±13.88 cm^3) when compared to healthy peers (37.17±8.46 cm^3; $p<0.05$). Similarly, bilateral volumes of FCF of pilocytic astrocytoma patients (23.45±9.95 cm^3) and of medulloblastoma patients (23.03±14.13 cm^3) were significantly smaller compared to healthy peers (36.47±13.82 cm^3; $p<0.05$).

In the medulloblastoma patients alone, the measurements showed significantly reduced values in patients with symptoms of CMS (group B, 17.1±11 cm^3) in comparison to those with no symptoms of CMS (group A, 32.51±12.28 cm^3; $p<0.01$).

Table 1 Volume of fronto-cerebellar fiber tracts given in cubic centimeters (cm^3) as mean±standard deviation (*$p<0.05$, **$p<0.001$ vs. CG, respectively)

Clinical outcome			
SIDE	Group A ($n=18$)	Group B ($n=11$)	HP ($n=10$)
Left	25.89±11.32	17.59±9.36**	37.17±8.46
Right	27.95±12.66	21.00±13.87	35.77±18.18
Both sides	26.92±11.88	19.29±11.68**	36.47±13.82
Histology			
SIDE	A ($n=14$)	E ($n=2$)	M ($n=13$)
Left	23.43±9.34*	24.58±7.31	21.71±13.88*
Right	23.47 ±10.89	44.53±2.78	24.35±14.81
Both Sides	23.45±9.95*	34.55±12.37	23.03±14.13*

Group A mainly clinically unaffected, *group B* with symptoms of PFS, *A* astrocytoma, *E* ependymoma, *M* medulloblastoma, *HP* healthy peers, *left/right* left/right cerebral hemisphere

Semiquantitative analysis of fiber signal intensity

Measurements of the cerebellar peduncles and the cerebellar structures are given in Table 2. For supratentorial structures, no significant differences were found between the patient groups. Fiber signal intensity in the left superior cerebellar peduncle of group B patients (0.90±0.54) was significantly lower than in healthy peers (1.55±0.53; $p<0.05$). This difference was even more pronounced when analyzing the right superior cerebellar peduncle (0.33±0.50 vs. 1.50±0.53, $p<0.001$). Medulloblastoma patients showed less fiber signal intensity in the same anatomical structure (left, 0.85±0.38; right, 0.54±0.52) than healthy peers (left, 1.55±0.53, $p<0.05$; right, 1.50±0.53, $p<0.01$), respectively (Table 2).

Signal intensity fiber bundles in the paravermal zone of both sides of group B patients were lower (left, 0.27±0.47; right, 0.09±0.30) when compared to healthy peers (left, 0.90±0.57, $p<0.05$; right, 0.70±0.67, $p<0.05$).

Pilocytic astrocytoma patients showed a significant lower signal of left side fiber bundles in the paravermal zone (0.07±0.27) in comparison to healthy peers (0.90±0.57; $p<0.001$). Similarly, the corresponding mean value of 0.08±0.28 of medulloblastoma survivors was significantly inferior when compared to healthy peers (0.90±0.57; $p<0.001$).

When analyzing the vermal and paravermal zone as midline cerebellar structures together, group A (0.23±0.51) as well as group B patients (0.10±0.30) had lower fiber intensity when compared to healthy peers (0.44±0.55; $p<0.01$ and $p<0.001$, respectively).

Fiber intensities in the midline cerebellar structures of both pilocytic astrocytoma (0.23±0.49) and medulloblastoma patients (0.19±0.39) were significantly smaller in comparison to healthy peers (0.49±0.56; $p<0.01$ and $p<0.001$, respectively).

Fractional anisotropy (FA)

We measured FA values in two frontal sections at the height of the foramen of Monro, an area where all subjects showed FCF signals. The ROI included the white matter in the vascular territory of the frontopolar artery, the frontal anteromedial artery, and the anterior limb of the internal capsule. FA was measured in the superior cerebellar peduncle and in the cerebellar midline structures (vermis and paravermal zone).

Group A (0.25±0.04; $p=0.001$) as well as group B patients (0.24±0.06; $p<0.01$) showed significant FA reduction in frontal white matter ROI when compared to healthy peers (0.28±0.04). Moreover, inferior FA was noted in the superior cerebellar peduncles in group A (0.23±0.06; $p<0.001$) as well as in group B patients (0.23±0.04; $p<0.01$) in comparison to healthy peers (0.29±0.04). Extent of CMS symptomatology did not correlate with FA measured in cerebellar midline structures.

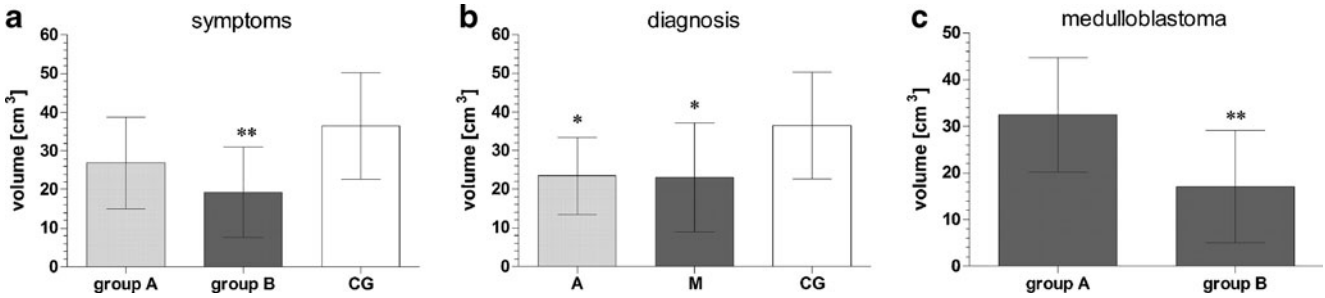

Fig. 3 Volumetric measurements of fronto-cerebellar fiber tracts. **a** Patients from group A (unaffected patients), group B (patients with symptoms of CMS), and the control group. **b** Patients with astrocytoma (*A*) diagnosis compared with the medulloblastoma (*M*) and control group (*CG*). **c** Medulloblastoma patients divided according to their postoperative symptoms of CMS to group A and group B (**$p<0.01$, *$p<0.05$; columns are given as mean±standard deviation)

Frontal ROIs of both pilocytic astrocytoma (0.25±0.04) and medulloblastoma patients (0.24±0.05) showed a statistically significant decrease of FA in comparison to healthy peers (0.28±0.04; $p<0.01$ for each group). In parallel, FA of the superior cerebellar peduncle of pilocytic astrocytoma (0.23±0.06; $p<0.01$) and medulloblastoma patients (0.24±0.05; $p<0.05$) was lower when compared to healthy peers (0.29±0.04). For ROIs of cerebellar midline structures, FA did not show any differences among the groups defined by histology.

Discussion

Visualization of fronto-cerebellar fiber tracts was achieved by using DTI in posterior fossa tumor patients as well as in healthy children. The measurement of FCF volumes may reveal an association with the extent of postoperative CMS symptoms as well as with medulloblastoma biology of pediatric cerebellar tumor survivors. Remarkably, this holds true for medulloblastoma patients showing less FCF volume if they were affected by CMS symptoms after surgery. Fiber intensity in the superior cerebellar peduncles as well as in cerebellar midline structures were diminished in children with postoperative CMS symptoms. Moreover, frontal white matter fractional anisotropy was inferior in patients compared to healthy peers. Thus, FCF integrity seems to show some relation to CMS after posterior fossa surgery, as anatomical substrate damage of regulatory pathways between the cerebellum and the frontal lobe may be linked to neurocognitive changes after posterior fossa surgery observed in CMS.

The pathomechanism of postoperative CMS injury is still subject of ongoing debates. Putative responsible anatomical structures for damage are the cerebellar vermis, brainstem, dentate nuclei, middle cerebellar peduncle, and superior cerebellar peduncle [12, 21, 23, 25]. In the largest prospective study, Robertson et al. found a negative correlation between tumor localization in the cerebellar hemispheres and the manifestation of CMS [25]. This reveals a positive correlation with cerebellar midline structures. An exclusive involvement of the vermis may be less likely since CMS has also been found in patients without damage to the cerebellar midline structures [9, 20, 35]. Siffert et al. demonstrated that avoidance of vermis splitting did not prevent the manifestation of the syndrome [30]. The latency of CMS onset in some cases argues against the hypothesis that only direct injury to anatomical structures is responsible. This delay may be explained by postsurgical edema, intraoperative manipulation, or subsequent ischemia due to vasospasm causing secondary damage to the sensitive neurocognitive circuitry [1, 33, 35]. Pollack et al. found a statistically significant correlation between cerebellar mutism and the occurrence of postoperative edema in the cerebellar peduncles [23]. Metabolic changes were found for clinical neurocognitive changes with some latency after posterior fossa surgery using SPECT imaging and MR spectroscopy [7, 8, 28]. The hypothesis that the latency of CMS manifestation is caused due to the time metabolic changes that evolve and an edema needs to spread is consistent with these findings.

Some recent neuroimaging studies indicated a correlation between disturbances of the dentatothalamocortical (DTC) outflow tracts with occurrence of CMS [16, 19, 34, 35]. The DTC pathways project towards the dentate nucleus of the cerebellum. They enter via the cerebellar peduncles into the brainstem and continue towards the contralateral thalamus and the prefrontal cortex [25], and may be a part of the FCF pathways visualized by DTI in this study. The fibers as well as the anatomical structures that we found to be relevant for CMS do include circuitry connections between the cerebellum to the prefrontal cortex similar to previous investigations [16, 19, 34, 35]. Since we used the frontal pole and the cerebellum as regions of interest to determine DTI fiber connections between the frontal cortex and cerebellar structures, we are not able to clearly distinguish between the anatomically described fiber connections described as dentatothalmocortical (DTC) as well as corticopontinecerebellar (CPC) fibers. We have to assume that DTI as performed in this study does pool together ascending (DTC) and descending tracts (CPC), and

Table 2 Semiquantitative measures of signal intensity graded in MR-DTI sections given as mean±standard deviation (grading scale—2=distinct area of fibers involving the anatomical area, 1=minimal area of fibers, 0=no fibers seen in the anatomical structure)

	Groups	Side	Superior cerebellar peduncle		Middle cerebellar peduncle		Vermis		Paravermal zone	
			IPSI	CONT	IPSI	CONT	Lob ant	Lob post	IPSI	CONT
Clinical	Group A (n=18)	Left	1.00±0.49	1.00±0.49	0.56±0.51	0.67±0.59	0.00±0.00	0.00±0.00	0.44±0.51	0.39±0.50
		Right	0.90±0.55	1.00±0.46	0.22±0.43	1.17±0.51	0.00±0.00	0.06±0.24	0.39±0.70	0.50±0.62
	Group B (n=11)	Left	0.90±0.54*	0.73±0.47	0.64±0.67	0.55±0.52	0.00±0.00	0.19±0.40	0.27±0.47*	0.18±0.40
		Right	0.33±0.50***	0.67±0.50	0.27±0.47	1.00±0.00	0.00±0.00	0.09±0.30	0.09±0.30*	0.27±0.47
	Healthy peers (n=10)	Left	1.55±0.53	1.00±0.47	1.00±0.67	0.80±0.63	0.13±0.35	0.40±0.52	0.90±0.57	0.50±0.53
		Right	1.50±0.53	1.10±0.74	0.50±0.71	1.00±0.82	0.00±0.00	0.20±0.42	0.70±0.67	0.60±0.52
Histology	Astrocytoma (n=14)	Left	1.00±0.55	0.93±0.62	1.14±0.53	0.71±0.61	0.00±0.00	0.07±0.27	0.07±0.27***	0.36±0.50
		Right	0.93±0.62	1.14±0.53	0.57±0.65	0.93±0.47	0.00±0.00	0.07±0.27	0.50±0.76	0.36±0.63
	Medulloblastoma (n=13)	Left	0.85±0.38*	0.85±0.38	1.00±0.00	0.46±0.52	0.00±0.00	0.08±0.28	0.08±0.28***	0.23±0.44
		Right	0.54±0.52**	1.00±0.00	0.54±0.52	0.62±0.51	0.00±0.00	0.08±0.28	0.08±0.28	0.38±0.51
	Healthy peers (n=10)	Left	1.55±0.53	1.00±0.47	1.00±0.67	0.70±0.48	0.13±0.35	0.40±0.52	0.90±0.57	0.50±0.53
		Right	1.50±0.53	1.10±0.74	0.50±0.71	1.00±0.82	0.00±0.00	0.20±0.42	0.70±0.67	0.60±0.52

Significant differences are found in the superior cerebellar peduncles as well as in the paravermal zone for both in group B and medulloblastoma patients versus healthy peers

Group A mainly clinically unaffected, *group B* with symptoms of CMS, *Lob* lobus, *ant* anterior, *post* posterior, *IPSI* ipsilateral, *CONT* contralateral

*p<0.05, **p<0.01, ***p<0.001 vs. healthy peers

may be interpreted independent to discrete anatomical structures. Thus, further studies are warranted to use ROIs, which are more specific for the anatomical pathways between the frontal lobe and the cerebellum like the pontine structures, dentate nuclei, and the thalamic nuclei, to further investigate the role of ascending and descending fiber tracts of being involved in the development of cerebellar mutism.

In the Robertson study, a positive correlation between tumor invasion into the brainstem and the development of CMS was found [25]. Moreover, McMillan and coworkers found brainstem compression as a predictor of CMS [16]. Similarly, Pollack et al. suggested the brainstem to be the neuroanatomical locus as the proximal portion of the DTC outflow tracts [16, 22, 23, 25]. The dentate nucleus cannot be identified with DTI, but its anatomical localization is included in the anatomical region graded as cerebellar midline structures. Also, injury to the cerebellar peduncles, corresponding to the findings in our study, has been theorized to be a causative factor [13, 16, 25].

Our findings showed diminished fiber intensity in the noted anatomical structures depending on tumor biology. Medulloblastoma patients showed a signal intensity decrease in the superior cerebellar peduncle and in the cerebellar midline structures in comparison to pilocytic astrocytoma patients. In addition, the decrease in patient group B was significant when compared to the healthy peers. These findings implicate that long-term outcome analysis need to be partially linked to protocols of adjuvant therapy. Symptoms of CMS are more often manifest in medulloblastoma patients, but are also observed in pilocytic astrocytoma patients treated with surgery alone, however with lower intensity. The increased likelihood that the syndrome occurs in medulloblastoma patients may be based on additional factors like different patterns of cell invasion, location of the tumor, and more significant risk of bleeding due to vascularization. In the literature, differences in tumor biology and therapy were alleged to contribute to incidence and extent of CMS [34]. Therapy protocols for medulloblastoma do include surgery, chemotherapy, and radiation, while pilocytic astrocytomas are treated by surgery alone. In our study, image data acquisition was performed in a considerable time after surgery. As limitation, we are not able to clearly distinguish between the effect of the surgery and any event within the further time course until imaging data collection, which includes the adjuvant therapy protocols. The use of chemotherapeutic agents and radiation do interfere with normal child brain development [33]. Therefore, the more pronounced damage to FCF structures observed in medulloblastoma patients may be attributed to adjuvant therapy. Interestingly, we were able to show that within the medulloblastoma patients who received similar adjuvant therapy, FCF volume was also significantly diminished if postoperative symptoms of CMS were reported. CMS, which primarily manifests within 1 to 2 days after surgery [25], is not caused by adjuvant therapy. Still, on the one hand adjuvant therapy may inhibit optimal recovery [34] and on the other CMS might cause long-lasting anatomical alterations, which might be represented in the FCF circuitry.

To further elucidate our findings of a diminished volume and fiber intensity in cerebellar midline structures and superior cerebellar peduncles in children who underwent fossa posterior surgery, we measured the FA values in relevant predefined ROIs of FCF. We found decreased FA values (loss of myelin integrity) in all patients in the frontal ROIs and the superior cerebellar peduncle. These findings corroborate the study of Rueckriegel et al. where FA values from medulloblastoma and pilocytic astrocytoma patients were found to be decreased compared to healthy peers [27]. In our study, FA value measurements did not differ between patient groups according to their clinical outcome. Supratentorial FA values were found to be significantly diminished in all pediatric cerebellar tumor survivor patients when compared to healthy peers. Rueckriegel et al. found differences in FA values not only between operated patients and healthy peers. Medulloblastoma patients after adjuvant therapy had a higher amount of voxels with significantly decreased FA than pilocytic astrocytoma patients [27]. In part, this may be attributed to a different analyzing algorithm. In our previous study, we used an analysis algorithm on a voxel-based comparison, whereas the current study used an averaged FA calculation within a specified ROI and a DTI based probabilistic approach for tractography. Major drawbacks of the probabilistic approach for tractography are based on computational estimation of fiber directions dealing with presence of noise within imaging acquisition [3]. However, since the acquired data reveal robust measurements for FCF and correlation with clinical as well as histological parameters, we support DTI-based tractography analysis as a valuable analysis tool in clinical studies.

In this context, DTI post-processed with fiber tracking algorithms is a promising tool to depict white matter tracts and possible pathological changes in vivo. Our study is the first to use DTI to measure fronto-cerebellar fibers in correlation with changes in the manifestation of CMS after fossa posterior surgery. DTI has been used previously to enter new perspectives in understanding CMS [11, 16]. However, one drawback of our study lies in the cross-sectional nature of its design. We used postoperative MRI images for fiber tracking and MRI datasets were recorded at a mean of 2.5 years after surgery. DTI image datasets were collected during follow-up for tumor control. Even more so, the damage to FCF detected after a relevant follow-up time after initial diagnosis confirms the significance of longer lasting structural changes after posterior fossa tumor removal. This holds especially true for the medulloblastoma cohort which showed FCF volume differences in postoperatively CMS

affected children compared to those without symptoms of CMS. In future studies, prospective DTI imaging pre- and postoperatively will be needed in order to confirm our study results concerning the pathogenesis of CMS and its relation to FCF circuitry. This may encounter organizational difficulties since DTI is not accessible in emergency situations or in short time frames after admission of a posterior fossa tumor patient. The current study is the basis for a step forward in understanding neurocognitive pathway disturbances in children. Our data may be helpful for future studies to prospectively analyze neurocognitive impairment in children with cerebellar tumor using DTI.

Conclusion

The current study investigated children after posterior fossa surgery using DTI fiber tracking analysis in order to analyze changes of fronto-cerebellar pathways in relation to postoperative symptoms of cerebellar mutism and tumor biology. We found significant lower volume measurements of FCF tracts and identified the superior cerebellar peduncle as well as the cerebellar midline structures as possible anatomical correlates for clinical impairment of CMS. Since these findings were seen within the medulloblastoma group of patients receiving similar adjuvant therapy, these findings seem to be independent of chemotherapy or radiation. DTI was found to be a valuable tool to investigate the underpinnings of neurocognitive changes after tumor therapy. Prospective studies need to further verify our findings.

References

1. Al-Anazi A, Hassounah M, Sheikh B, Barayan S (2001) Cerebellar mutism caused by arteriovenous malformation of the vermis. Br J Neurosurg 15(1):47–50
2. Catsman-Berrevoets CE, Van Dongen HR, Mulder PG, Paz y Geuze D, Paquier PF, Lequin MH (1999) Tumour type and size are high risk factors for the syndrome of "cerebellar" mutism and subsequent dysarthria. J Neurol Neurosurg Psychiatry 67(6):755–757
3. Chung HW, Chou MC, Chen CY (2011) Principles and limitations of computational algorithms in clinical diffusion tensor MR tractography. AJNR Am J Neuroradiol 32(1):3–13
4. Crutchfield JS, Sawaya R, Meyers CA, Moore BD 3rd (1994) Postoperative mutism in neurosurgery. Report of two cases. J Neurosurg 81(1):115–121
5. De Smet HJ, Baillieux H, Catsman-Berrevoets C, De Deyn PP, Mariën P, Paquier PF (2007) Postoperative motor speech production in children with the syndrome of "cerebellar" mutism and subsequent dysarthria: a critical review of the literature. Eur J Paediatr Neurol 11(4):193–207
6. Doxey D, Bruce D, Sklar F, Swift D, Shapiro K (1999) Posterior fossa syndrome: identifiable risk factors and irreversible complications. Pediatr Neurosurg 31(3):131–136
7. Erşahin Y, Yararbas U, Duman Y, Mutluer S (2002) Single photon emission tomography following posterior fossa surgery in patients with and without mutism. Childs Nerv Syst 18(6–7):318–325
8. Erşahin Y (1998) SPECT in cerebellar mutism. Childs Nerv Syst 14(11):611–613
9. Erşahin Y (1998) Is splitting of the vermis responsible for cerebellar mutism? Pediatr Neurosurg 28(6):328
10. Gelabert-González M, Fernández-Villa J (2001) Mutism after posterior fossa surgery. Review of the literature. Clin Neurol Neurosurg 103(2):111–114
11. Gudrunardottir T, Sehested A, Juhler M, Grill J, Schmiegelow K (2011) Cerebellar mutism: definitions, classification and grading of symptoms. Childs Nerv Syst 27(9):1361–1363
12. Koh S, Turkel SB, Baram TZ (1997) Cerebellar mutism in children: report of six cases and potential mechanisms. Pediatr Neurol 16(3):218–219
13. Kotil K, Eras M, Akçetin M, Bilge T (2008) Cerebellar mutism following posterior fossa tumor resection in children. Turk Neurosurg 18(1):89–94
14. Krainik A, Lehéricy S, Duffau H, Capelle L, Chainay H, Cornu P, Cohen L, Boch AL, Mangin JF, Le Bihan D, Marsault C (2003) Postoperative speech disorder after medial frontal surgery: role of the supplementary motor area. Neurology 60(4):587–594
15. Le Bihan D, Mangin JF, Poupon C, Clark CA, Pappata S, Molko N, Chabriat H (2001) Diffusion tensor imaging: concepts and applications. J Magn Reson Imaging 13(4):534–546
16. McMillan HJ, Keene DL, Matzinger MA, Vassilyadi M, Nzau M, Ventureyra EC (2009) Brainstem compression: a predictor of postoperative cerebellar mutism. Childs Nerv Syst 25 (6):677–681
17. Mochizuki H, Saito H (1990) Mesial frontal lobe syndromes: correlations between neurological deficits and radiological localizations. Tohoku J Exp Med 161(Suppl):231–239
18. Morris EB, Phillips NS, Laningham FH, Patay Z, Gajjar A, Wallace D, Boop F, Sanford R, Ness KK, Ogg RJ (2009) Proximal dentatothalamocortical tract involvement in posterior fossa syndrome. Brain 132(Pt 11):3087–3095
19. Nagaratnam N, Nagaratnam K, Ng K, Diu P (2004) Akinetic mutism following stroke. J Clin Neurosci 11(1):25–30
20. Nishikawa M, Komiyama M, Sakamoto H, Yasui T, Nakajima H (1998) Cerebellar mutism after basilar artery occlusion—case report. Neurol Med Chir (Tokyo) 38(9):569–573
21. Ozgur BM, Berberian J, Aryan HE, Meltzer HS, Levy ML (2006) The pathophysiologic mechanism of cerebellar mutism. Surg Neurol 66(1):18–25
22. Pollack IF (1997) Posterior fossa syndrome. Int Rev Neurobiol 41:411–432
23. Pollack IF, Polinko P, Albright AL, Towbin R, Fitz C (1995) Mutism and pseudobulbar symptoms after resection of posterior fossa tumors in children: incidence and pathophysiology. Neurosurgery 37(5):885–893
24. Rekate HL, Grubb RL, Aram DM, Hahn JF, Ratcheson RA (1985) Muteness of cerebellar origin. Arch Neurol 42(7):697–698
25. Robertson PL, Muraszko KM, Holmes EJ, Sposto R, Packer RJ, Gajjar A, Dias MS, Allen JC; Children's Oncology Group (2006) Incidence and severity of postoperative cerebellar mutism syndrome in children with medulloblastoma: a prospective study by the Children's Oncology Group. J Neurosurg 105(6 Suppl):444–451
26. Rønning C, Sundet K, Due-Tønnessen B, Lundar T, Helseth E (2005) Persistent cognitive dysfunction secondary to cerebellar injury in patients treated for posterior fossa tumors in childhood. Pediatr Neurosurg 41(1):15–21
27. Rueckriegel SM, Driever PH, Blankenburg F, Lüdemann L, Henze G, Bruhn H (2010) Differences in supratentorial damage of white matter in pediatric survivors of posterior fossa tumors with and

without adjuvant treatment as detected by magnetic resonance diffusion tensor imaging. Int J Radiat Oncol Biol Phys 76 (3):859–866
28. Rueckriegel SM, Bruhn H, Hernaiz D (2012) Supratentorial neurometabolic alterations in pediatric survivors of posterior fossa tumors. Int J Radiat Oncol Biol Phys 82(3):1135–1141
29. Schmahmann JD, Shermann JC (1997) Cerebellar cognitive affective syndrome. Int Rev Neurobiol 41:433–440
30. Siffert J, Poussaint TY, Goumnerova LC, Scott RM, LaValley B, Tarbell NJ, Pomeroy SL (2000) Neurological dysfunction associated with postoperative cerebellar mutism. J Neurooncol 48(1):75–81
31. Sommer M, Koch MA, Paulus W, Weiller C, Büchel C (2002) Disconnection of speech-relevant brain areas in persistent developmental stuttering. Lancet 360(9330):380–383
32. Tahta K, Cirak B, Pakdemirli E, Suzer T, Tahta F (2007) Postoperative mutism after removal of an anterior falcine meningioma. J Clin Neurosci 14(8):793–796
33. Turgut M (2007) Re: The pathophysiologic mechanism of cerebellar mutism (Ozgur et al. Surg Neurol 2006;66:18–25). Surg Neurol 68(1):117
34. Wells EM, Walsh KS, Khademian ZP, Keating RF, Packer RJ (2008) The cerebellar mutism syndrome and its relation to cerebellar cognitive function and the cerebellar cognitive affective disorder. Dev Disabil Res Rev 14(3):221–228
35. Wells EM, Khademian ZP, Walsh KS, Vezina G, Sposto R, Keating RF, Packer RJ (2010) Postoperative cerebellar mutism syndrome following treatment of medulloblastoma: neuroradiographic features and origin. J Neurosurg Pediatr 5(4):329–334